

Towards an Accurate Modeling of Frequency-Dependent Wind Farm Components under Transient Conditions

M. A. Abd-Allah, Mahmoud N. Ali, A. Said

Faculty of Engineering at Shoubra, Benha University, Egypt

Article Info

Article history:

Received Mar 2, 2014

Revised Jul 10, 2014

Accepted Jul 23, 2014

Keyword:

ATP/EMTP

FFT

GPR

Surge arrester model

Transient response

WTs

ABSTRACT

Frequency dependence complete model is set up for describing the lightning transient behavior of the wind turbines (WTs). To get an appropriate wind turbine model, a high frequency models of surge arrester protecting the boost transformer, transformer and ground electrode soil ionization are implemented. The transient responses and Ground Potential Rise (GPR) can be obtained at different locations in the WT's and connected grid in the time domain as well as in the frequency domain using Fast Fourier Transform (FFT). To check the validity of the model, Surge arresters protection level at different locations, at i.e. LV, MV and HV, is compared with ABB manufacture data sheet, Also a comparison has been made between simple and frequency dependence model of overall wind farm components using ATP/EMTP. This paper provides an accurate simulation of wind farm components under transient condition.

*Copyright © 2014 Institute of Advanced Engineering and Science.
All rights reserved.*

Corresponding Author:

M. A. Abd-Allah,

Faculty of Engineering at Shoubra, Benha University, Egypt.

Email: abdelrahman.ghoniem@feng.bu.edu.eg

1. INTRODUCTION

With a rapid growth in wind power generation, lightning hazard to wind turbines (WTs) has come to be regarded with more attention. Due to their great height, distinctive shape, and exposed location, WT's are extremely vulnerable to lightning stroke. After a WT is struck by lightning, high lightning current flows through the WT and causes considerable damage to electrical equipment inside the WT structure and wind turbine nacelle results stop of the generator operation and probably expensive repairs [1].

In order to decrease downtime, repairs and blade damaged. Protecting the blade is very important and well-designed lightning protection is a necessity for this equipment so Modern wind turbine blades are made of insulating materials such as glass fibre reinforced plastic (GFRP) as a common material or wood epoxy. The lightning protection of wind turbine blades can be classified as receptor, metallic cap, mesh wire, and metallic conductor as reported in IEC-61400-24 standards.

In general, the problem of lightning protection of wind turbine blades is to conduct the lightning current safely from the attachment point on the blade to the hub and then to the ground.

However another serious problem known as "back-flow surge" which not only causes damages to the wind turbine that has been struck but also the other turbines that have not. The back-flow surge phenomenon has been defined as the surge flowing from a customer's structure such as a communication tower into the distribution line. High resistivity soil often makes Surge Arresters (SAs) at tower earthing systems operate in reverse and allow backflow of surge current to the grid. The phenomenon of surge invasion from a wind turbine that is struck by lightning to the distribution line in a wind farm is quite similar to the case of "back-flow surge" [2].

Due to significant influence on the wind farm behavior under lightning, the transient response must be either accurately measured which very expensive and time consuming or reliably predicated by simulations which allowing for parametric studies and optimization. Up till now the predominant approach

for simulating transient due to lightning is based on the representation of the wind farm components by their equivalent circuits. Performance of wind farm under lightning requires accurate modeling of its components. So in this paper wind farm is implemented using high frequency models components as SA, Transformer and ground electrode to integrally describe this lightning current path. Validation of these models and computation, characteristics and hazards of back-flow surge in wind farm are analyzed using onshore wind farm as an example.

2. DESCRIPTION OF THE INVESTIGATED ONSHORE WIND FARM:

Figure1. Shows layout of onshore wind farm composed of two identical wind power generators. Boost transformers for the generators are installed in vicinity of the wind turbine towers. All boost transformers are connected to the grid via grid-interactive transformer by overhead distribution line. Surge arresters are inserted to the primary and secondary sides of the boost and grid-interactive transformers.

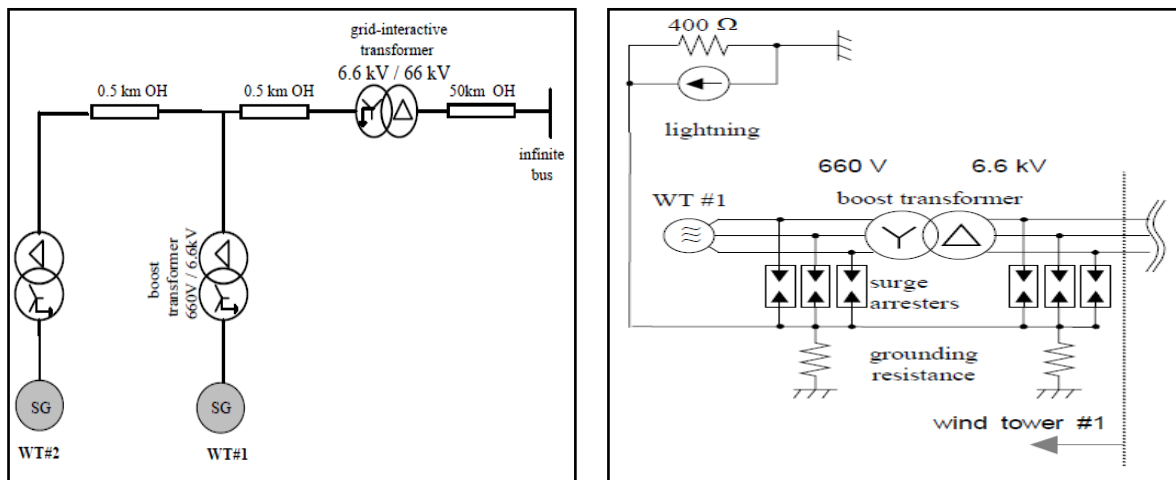


Figure 1. Wind farm model [2]

3. MODELING OF THE ELECTRIC COMPONENTS OF THE ONSHORE WIND FARM USING ATP/EMTP:

In this section, the detailed high frequency modeling of the electric components of the onshore wind farm using the ATP/EMTP is demonstrated. These components include Transmission line (TL), transformers, power system grid and surge arresters.

3.1. Lightning Model:

In order to simulate the impact of lightning current on power system or its components with convenience, the lightning current in the mode of mathematical function is usually represented. After the long-term speculation and research by many researchers, the approximate mathematical function was proposed. A current function model called Heidler is now used widely [3, 4, 5]. A 400 Ω lightning path resistance was parallelly connected to simulate natural lightning. Equation (1) represent the lightning current, waveform of 51kA-2/631μs is used in this study as shown in Figure 2. The waveform of Heidler lightning current is simulated by ATP/EMTP software.

$$i(t) = I_o \frac{(t/\tau_1)^2}{[(t/\tau_1)^2 + 1]} e^{-t/\tau_2} \quad (1)$$

Where

I_0 : the peak of current

τ_1, τ_2 : time constants of current rising and dropping

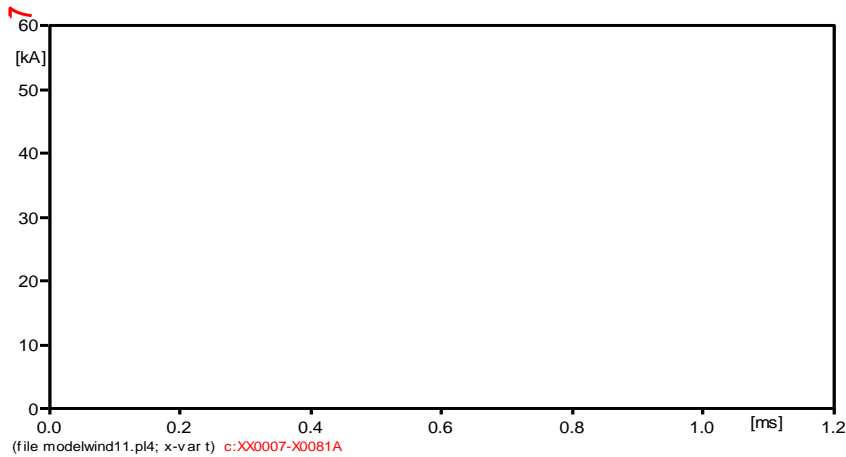


Figure 2. The Waveform of 51ka - 2/631 μ s Lightning Current

3.2. Wind Turbine Generator:

Table 1 gives the required data for modeling the generators of the wind turbines, transmission line and transformers.

Table 1 a, b, c. Wind Turbines, Transformers Data and connected line data [2]

Wind Turbine Model(Synchronous Generator- Y connected)	
Voltage (line rms)	0.660 [kV]
Rated power	1.0 [MVA]
Leakage reactance	0.1 [H]
Frequency	60.0 [Hz]
Transformer Model (Boost, Grid-Interactive)	
Connection method	Y / Δ , Y / Δ
Voltage (line rms)	0.660/6.6 [kV], 66.0/6.6 [kV]
Rated power	1.0 [MVA], 10.0 [MVA]
Leakage reactance	0.15 [p.u]
Copper losses	0.005 [p.u]
No-load losses	neglected
Line Model (values at 60 Hz)	
positive / zero phase resistance [Ω /Km]	0.00105/0.021
Positive / zero phase inductance [mH/Km]	0.83556/2.50067
Positive / zero phase capacitance [nF/Km]	12.9445/6.4723

3.3. Wind Turbine Blades and Towers:

The down conductor in the blade and the wind turbine tower have been considered as a lossless transmission line and they were estimated according to following experimental equation [4, 5, 6, 7], where the down conductor and the tower often were treated as a cylindrical conductor. Equation (2) represents the characteristic impedance of tower and the blade.

$$Z = 60 \left(\ln \frac{2\sqrt{2}}{r} h - 2 \right) \quad (2)$$

Where, Z is the surge impedance, r and h are the cylinder radius and height, respectively. The wind tower is taken as an iron vertical conductor of 60 m height and 3.0 m radius.

3.4. Transmission Lines and cables:

The overhead lines are considered and represented by single-phase positive wave impedance (i.e. Surge impedance) with the light velocity.

$$Z_0 = \sqrt{L/C} \quad \Omega \quad (3)$$

$$v = \frac{1}{\sqrt{LC}} \quad m/s \quad (4)$$

Where, C and L are the capacitance and inductance of line, respectively, Z_0 is the surge impedance and v is the propagation velocity [3, 8].

3.5. Transformer:

In order to study the transient involving frequencies up to a few kHz, stray capacitance of transformer coils must be added to the transformer model. Capacitances are actually distributed, but lumped parameters at the winding terminals for the total capacitance can be used with reasonable accuracy in this case [3, 8, 9]. However, the transformer capacitances are often difficult to be determined. Transformer capacitance is represented by C_H , C_L and C_{HL} as shown in Figure 3 Where, C_H is the capacitance of high winding to ground, C_L is the capacitance of low winding to ground and C_{HL} is the capacitance between high and low windings. Normally the C_L and C_{HL} are greater than C_H . This is because the fact that the high voltage calls for more separation between windings and between windings and core. The present work considers these capacitances as in a table 2 [3].

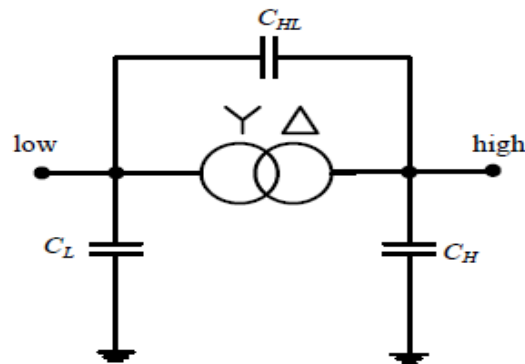


Figure 3. High Frequency Transformer Model.

Table 2. Typical Capacitance of Transformers (Capacitance in nF) [3]

Transformer MVA	Core Type		
	C_H	C_{HL}	C_L
1	1.2-14	1.2-17	3.1-16
2	1.4-16	1-18	3-16
5	1.2-14	1.1-20	5.5-17
7	2.7-11	3.5-17	8-16
10	4-7	4-11	8-18
25	2.8-4.2	2.5-18	5.2-20

3.6. Surge Arrester:

Surge arrester devices play an important role for mitigating the overvoltage due to lightning, switching. Under both normal and abnormal conditions, the arrester handles its operation based on its nonlinearity, i.e. V-I characteristics [9].

A simplified model was derived from IEEE model [10, 11]. The model circuit is shown in Figure 4. This model is composed by two sections of nonlinear resistances usually designated by A_0 and A_1 which are separated by inductance L_1 and L_0 . A parallel resistance R_p (about 1 MΩ) is added to avoid the numerical instability of the combination of the current source and nonlinear elements. This model has the same operating principles as the IEEE model. The main advantage of this model is that the parameters were determined using only the electrical data and did not take into consideration any physical characteristics of the surge arrester [12].

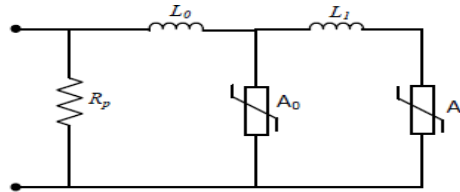


Figure 4. Pinceti and Giannettoni model

In case medium and high voltage levels the inductances L_1 and L_0 in the model are in μH and calculated using:

$$L_1 = \frac{1}{4} \frac{Ur1/T2 - Ur8/20}{Ur8/20} U_n \tag{5}$$

$$L_0 = \frac{1}{12} \frac{Ur1/T2 - Ur8/20}{Ur8/20} U_n \tag{6}$$

In case low voltage levels the inductances L_1 and L_0 in the model are in μH and calculated using:

$$L_1 = 0.03 U_n \tag{7}$$

$$L_0 = 0.01 U_n \tag{8}$$

Where U_n is the arrester rated voltage in kV, $Ur1/T2$ is the residual voltage at 10 kA fast front current surge (1/T2 μs). $Ur8/20$ is the residual voltage at 10 kA current surge with 8/20 μs time parameters.

The nonlinear characteristics of the two elements A_0 and A_1 are based on the pu data published in [13] and the corresponding nonlinear characteristics of A_0 and A_1 are shown in Figure 6.

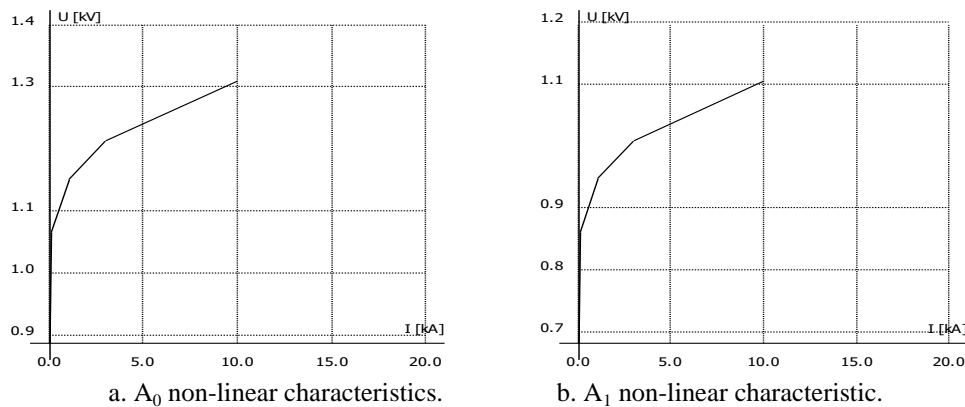


Figure 6. Surge Arrester Elements Nonlinear Characteristics.

The surge arrester model is simulated and tested using ATP/EMTP circuit shown in Figure 7.

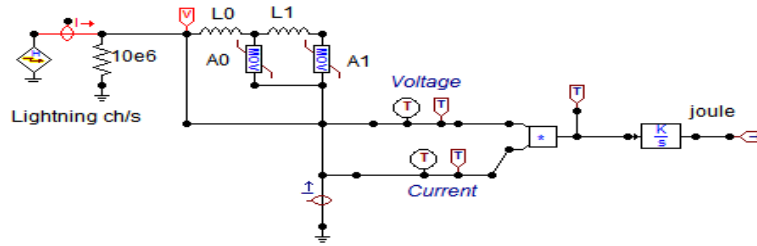


Figure 7. ATP/EMTP Circuit for Surge Arrester.

The arrester model is tested to match the manufacture's data sheet [14] under switching and lightning characteristics. 440kV SA with L_1 and L_0 are equal $0.07\mu\text{H}$ [6] used in low voltage side boost transformer. A discharge current 8/20 μs , 5 kA and 25 kA for nominal and maximum conditions respectively are injected to the surge arrester. The error of residual voltage rather than the manufactured data is found 0.22% at the nominal discharge current and -1.7% at the maximum discharge current. This error is computed as $(\text{Ups-Up})/\text{Up}$, where Ups is simulated residual voltage (the simulated voltage protection level). The injected current, the residual voltage and the absorbed energy are as shown in Figures 8 and 9 for nominal and maximum discharge currents, respectively.

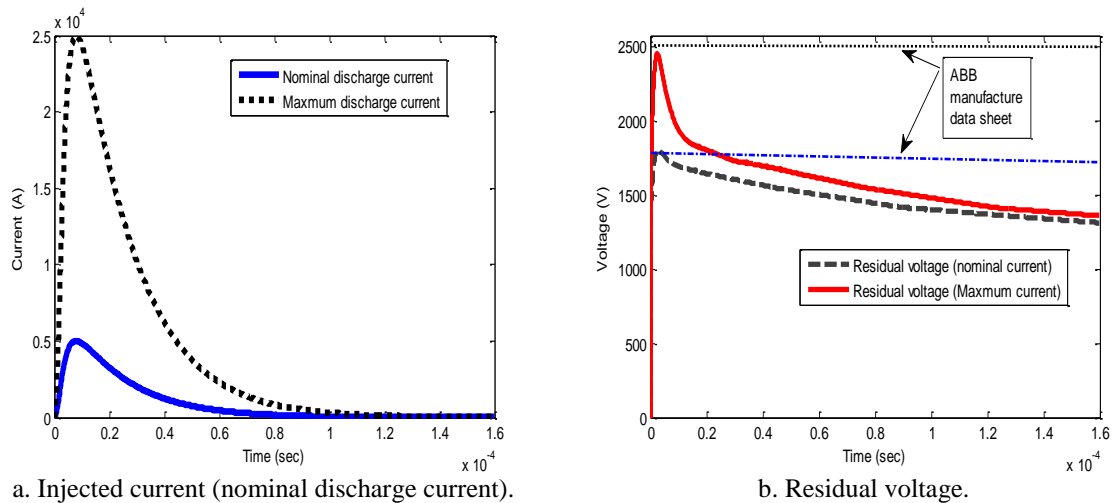


Figure 8. Injected nominal and maximum discharge current and residual voltage.

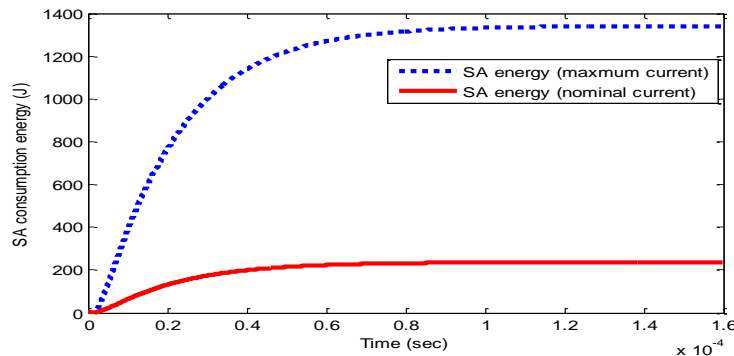


Figure 9. Absorbed Energy under Injected Nominal and Maximum Discharge Current.

The MV surge arrester protecting boost transformer with L_1 and L_0 are $0.0952 \mu\text{H}$ and $0.286 \mu\text{H}$ respectively [6].from test as shown in Figure 10 find errors within acceptable limits

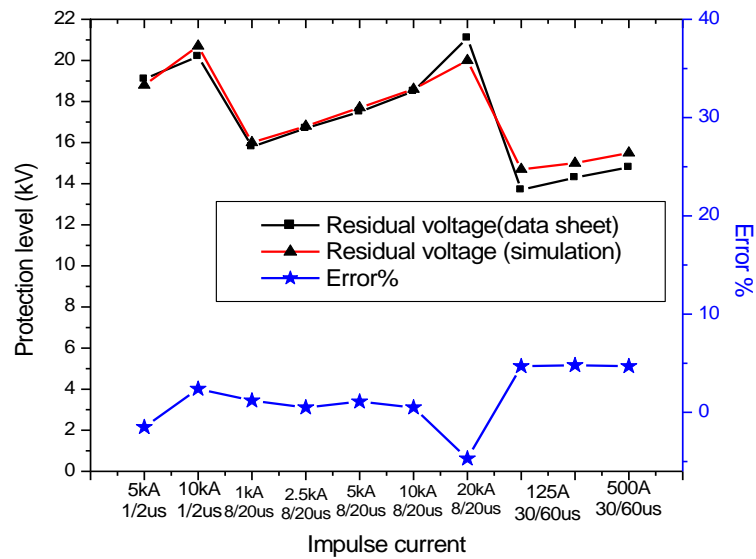


Figure 10. MVSA Validation

The HV surge arrester protecting grid transformer with L_1 and L_0 are $1.62\mu\text{H}$ and $0.54\mu\text{H}$ respectively. From test as shown in Figure 11 find errors within acceptable limits

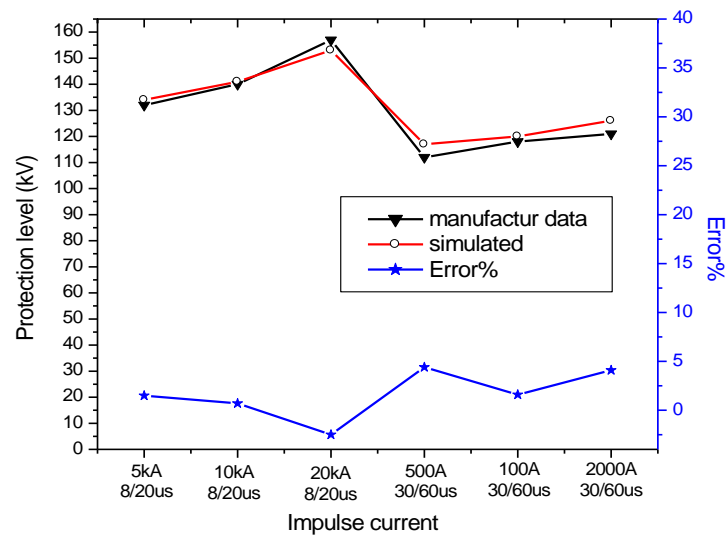


Figure 11. HVSA Validation

3.7. Vertical ground rod modeling:

Grounding systems behavior is well understood at power frequency. However, during lightning strokes the grounding systems performance might be different. The waveform of the lightning current has a major influence on the dynamic performance of ground electrodes. While high lightning current intensity improves the dynamic grounding performance due to ionization of the soil. In case of high lightning currents the electric field at the ground electrodes might become larger than the electric strength of the soil. Which can cause breakdown and sparks discharge in the soil. This phenomenon improves the grounding system

performance so its ignoring always gives inaccurate results. On the other hand, due to the frequency dependent phenomena, the grounding performance might be much worse during fast front lightning current pulses. This can deteriorate the efficiency of the protection. Grounding system of a wind turbine plays a critical role, since overvoltages caused by lightning strikes and other faults has to be successfully dispersed into the ground. So, it is important to get an accurate model of the wind turbine grounding system. In this paper the behavior of the wind turbine under lightning strikes has been studied using two different models for the grounding resistance [15]. The first model is the linear model of grounding resistance which is based on a constant value for the grounding resistance i.e. low voltage, low frequency [16]. The constant resistance R_0 of the model is estimated in ohm based on the rod dimensions and the soil parameters [15]:

$$R_0 = \frac{\rho}{2\pi l} \left\{ \ln \frac{4l}{a} - 1 \right\} \quad (9)$$

Where, ρ is the soil resistivity ($\Omega \cdot m$), L is the electrode length (m) and a is the electrode radius (m).

The other model is based on the nonlinear performance of the grounding resistance with high currents i.e. high voltage, high frequency [16]. The nonlinearity nature of the ground resistance can be represented by a nonlinear resistance, R_t , whose value is given as [15];

$$\begin{cases} R_t = R_0 \rightarrow \text{For}(i < I_g) \\ R_t = \frac{R_0}{\sqrt{1 + \frac{i}{I_g}}} \rightarrow \text{For}(i \geq I_g) \end{cases} \quad (10)$$

Where, i is the current through the rod (kA), and I_g is the critical current for soil ionization (kA) which is given by:

$$I_g = \frac{E_0 * \rho}{2\pi R_0^2} \quad (11)$$

Where, E_0 is the critical soil ionization gradient.

4. MODEL VALIDATION:

In this study, the wind power generator modeled as a synchronous machine for simplicity. The grounding model at each wind tower is simulated as three separated ground electrodes, where each electrode simulated as 10Ω resistance. There is no connection between the grounding systems for wind turbines. The distribution line is assumed as overhead line and simulated as transposed distributed line parameters. The lightning stroke is taken as striking wind turbine (WT#1) as shown in Figure 12.

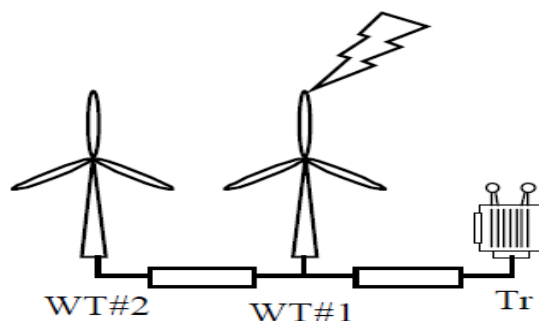


Figure 12. Lightning hit WT#1 [3]

4.1. Effect Of Frequency Dependant Surge Arrester and Transformers Model on Back Flow Current Overvoltages:

In this work, The backflow current-overvoltages is evaluated using different transformer and surge arrester models in the time domain as well as frequency domain using Fast Fourier Transform (FFT) considering onshore wind farm. Case#1 Simple model of SA consists of only one non linear element with characteristics and Power frequency transformer model as shown in figure 13.

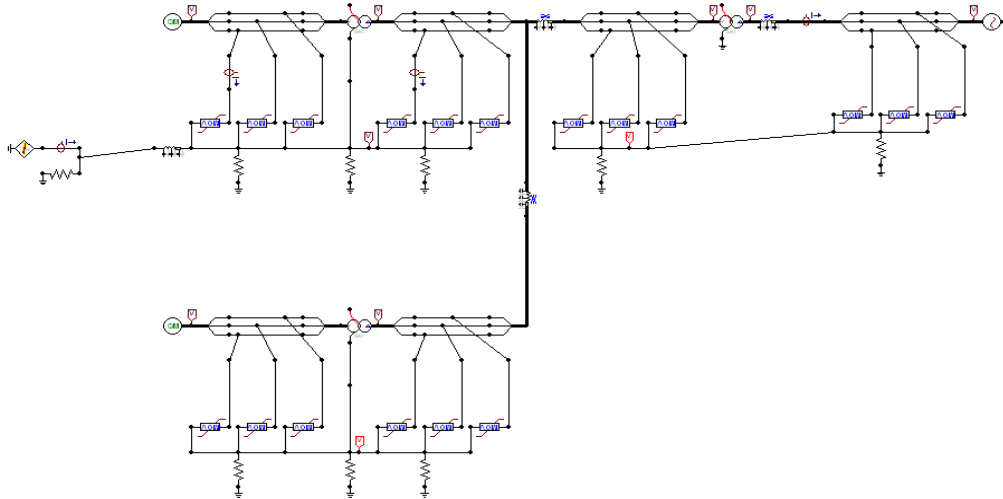


Figure 13. Atpdraw Circuit of Two Wind Turbines with Simple Model

Case#2 frequency dependent transformer model and frequency dependent model of SA is a combination of non linear elements and linear inductances which provides dynamic behavior during lightning. The SAs are used at low, medium and high voltage levels in the wind farm as shown in figure 14.

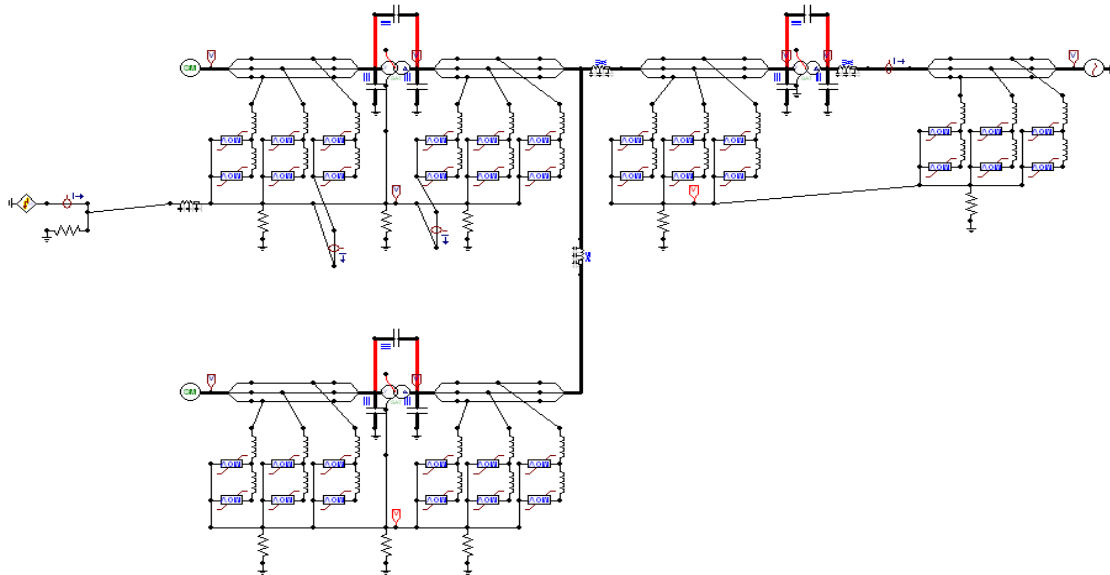
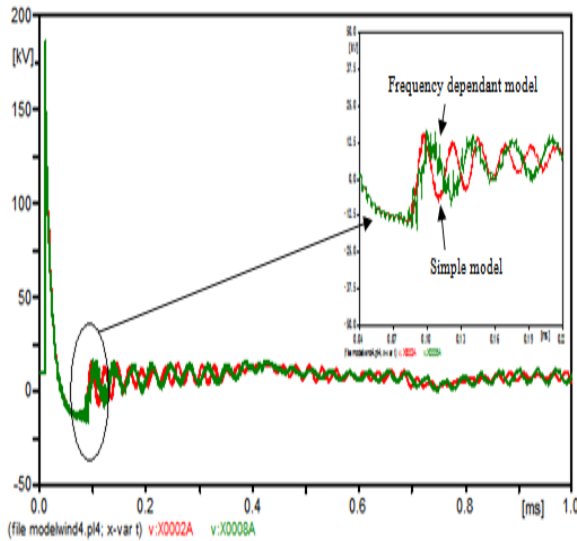


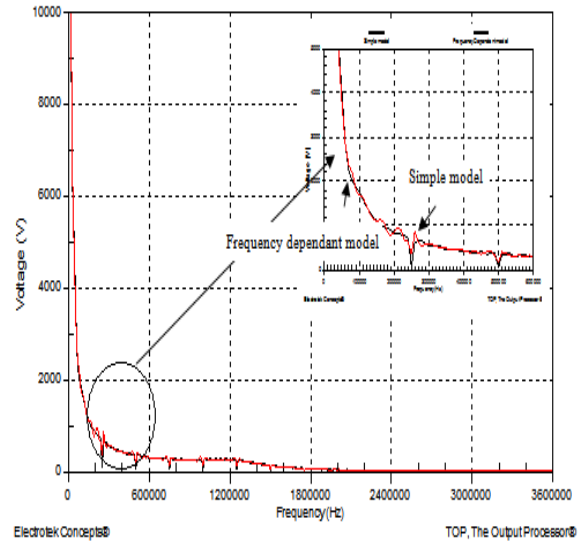
Figure 14: Atpdraw Circuit of Two Wind Turbines with Freq. Dependant Model

Figures 15 to 18 show the voltage waveforms, peak value, and frequency spectrum oscillation comparison at different locations of the wind farm. In different two cases, i.e. Simple and frequency dependent model, It is observed that the peak magnitude of the generated overvoltage at WT#1 generator terminal reach to 200kV, at (WT#1) boost transformer secondary side reach to 186kV, at (WT#2) boost

transformer secondary side reach to 25kV and at grid reach to 28kV in different models. It is clear that small change in peak value of overvoltages under simple and frequency dependant model. But from frequency content point of view, it can be seen that the amplitude voltage at different frequencies when using simple model is higher than that when using frequency dependant model. This can be attributed to the fact that the reflecting traveling waves at junction of the boost transformer of WT#2 and at the junction of the grid-interactive transformer are decreased due to the presence of the capacitors in the frequency dependant model. On the other hand, the frequency dependent model considers very high impedance at high frequencies. Therefore, for a better surge analysis of wind farm, the capacitance between winding of transformer model must be taken to get accurate transient results.

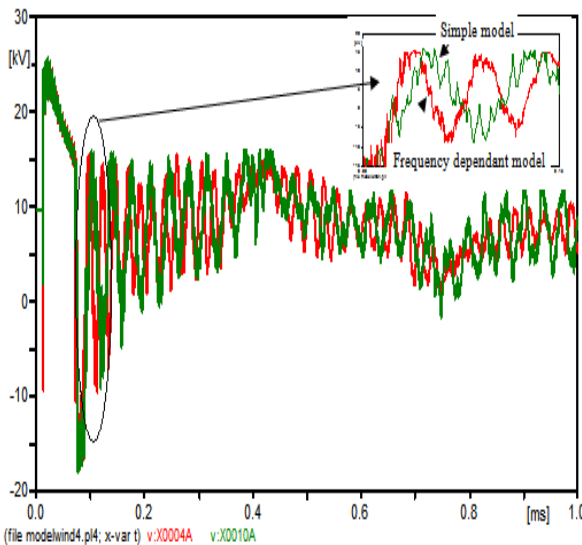


A. Waveforms Comparison @Wt#1 In Case Simple and Frequency Dependant Model

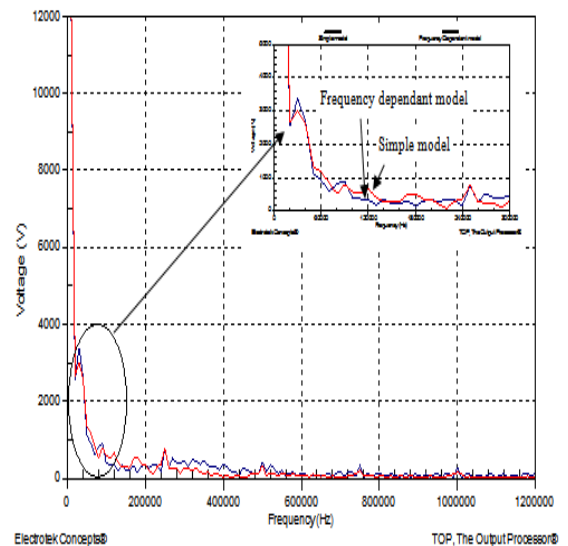


B. Frequency Spectrum Comparison

Figure 15. Overvoltages and Frequency Spectrum @WT#1

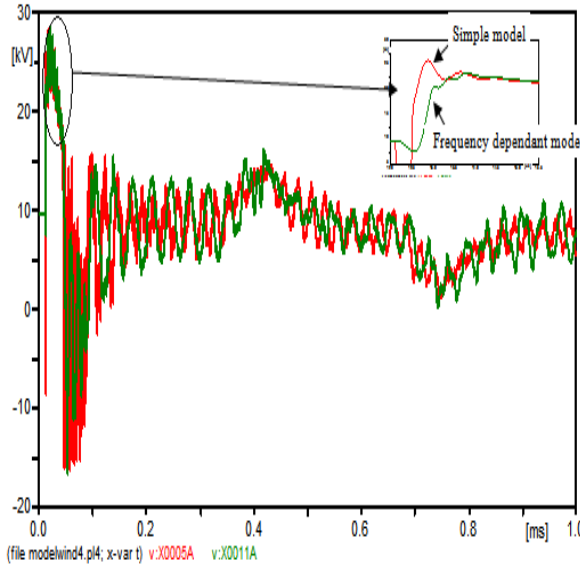


c. Waveforms Comparison @WT#2 In Case Simple And Frequency Dependant Model

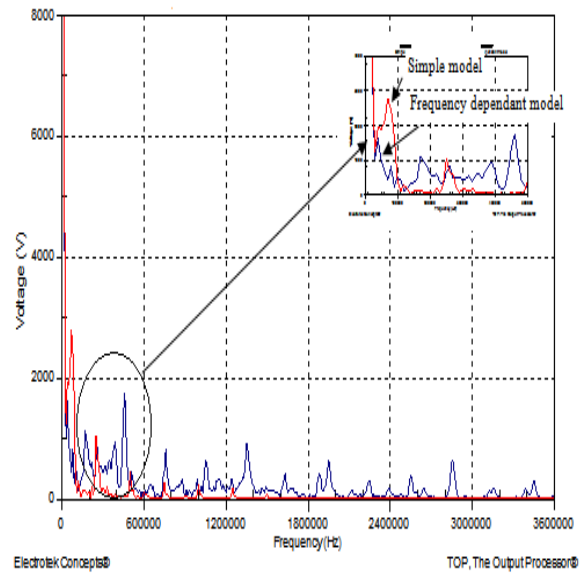


d. Frequency Spectrum Comparison

Figure 16. Overvoltage and Frequency Spectrum @WT#2



c. Waveforms Comparison at Grid In Case Simple and Frequency Dependant Model



d. Frequency Spectrum Comparison

Figure 17. Overvoltage And Frequency Spectrum At Grid

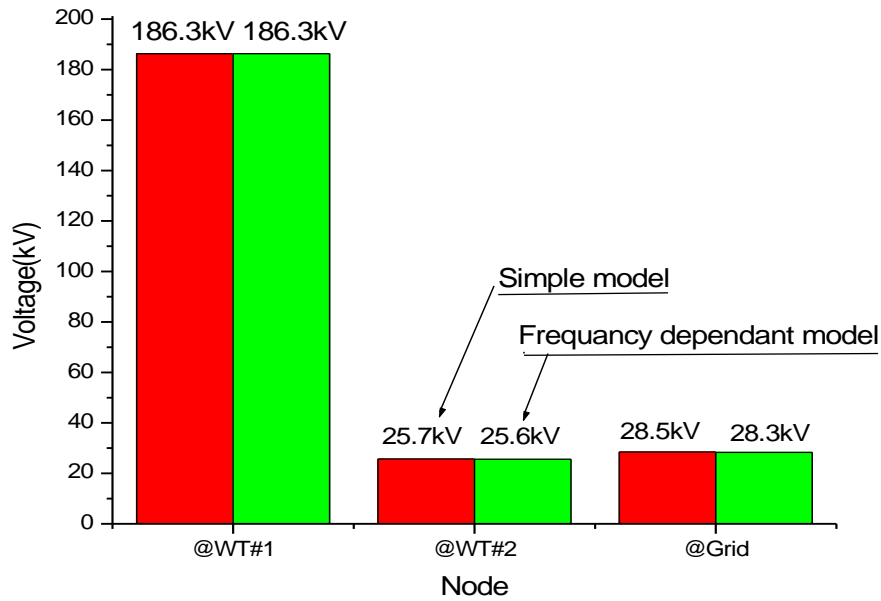


Figure 18. Overvoltage Peak Comparisons At Each Node Under Different Cases

4.2. Effect of Vertical Ground Rod Modeling:

In this work, each wind turbine is grounded using three vertical rods each rod has a length of (3 m) with diameter of (2.54 cm). Assuming that the spacing between these rods is large and enough to neglect the interaction between them. The soil parameters are taken as $\rho=100 \Omega.m$, $\epsilon_r=8$ and $\mu_r=1$ [14]. Figures 19 to 27 show comparison of voltage wave forms and GPR with varying grounding model (constant resistance and non linear resistance). The results show that the ground model is significant effect on the maximum GPR and overvoltage peak value. The GPR and overvoltage peak value is low when the soil ionization effect is

considered (nonlinear resistance model). This can be attributed that when the lightning current through the grounding rods exceeds the critical value, i.e. $I_g=5.5\text{KA}$, the grounding resistance is decreased where the current in the grounding rods is high. On the other hand, the maximum value of the GPR is high when using the constant resistance. This is because that the soil ionization is not considered in this model. Therefore, the soil ionization effect is an important factor and should be considered for transient studies especially in lightning study.

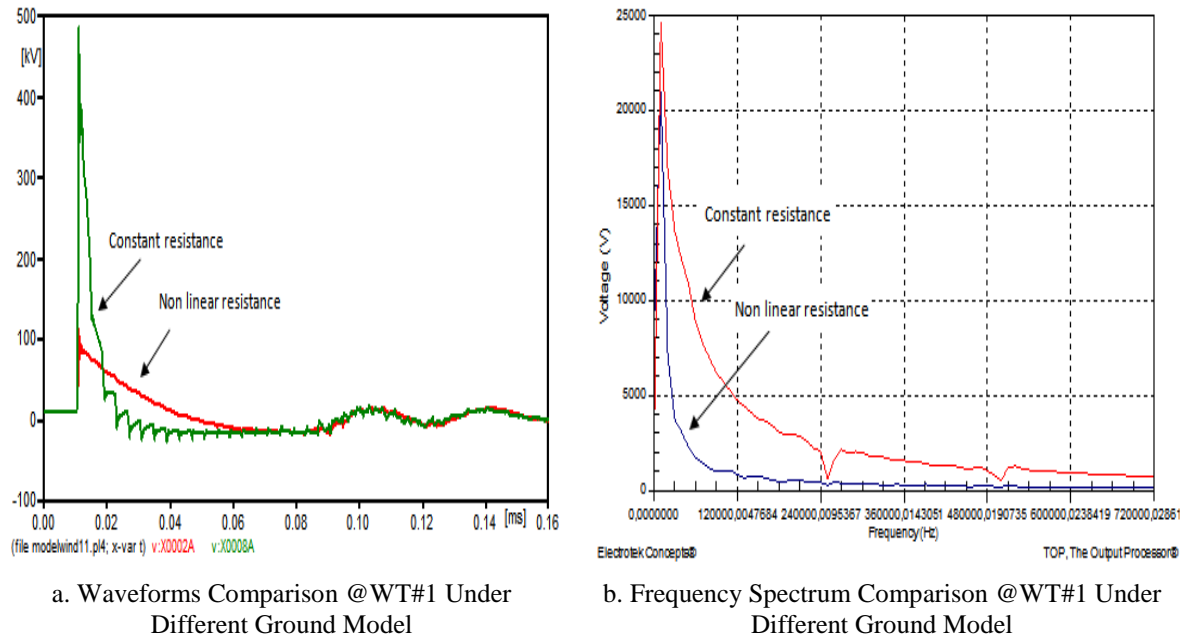


Figure 19. Overvoltage and Frequency Spectrum @WT#1

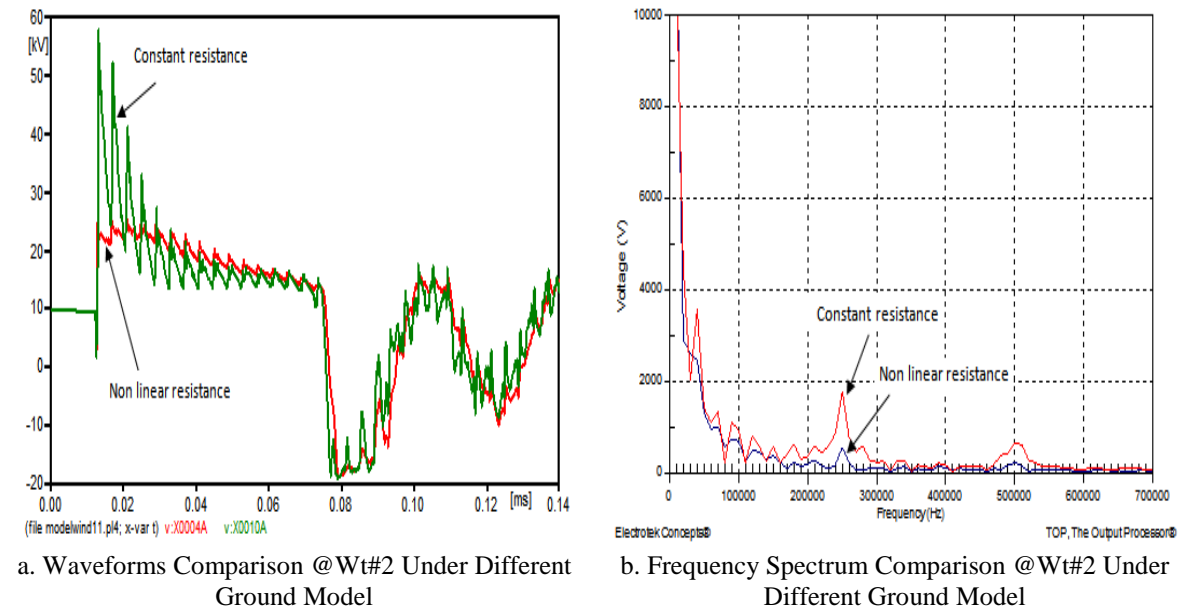
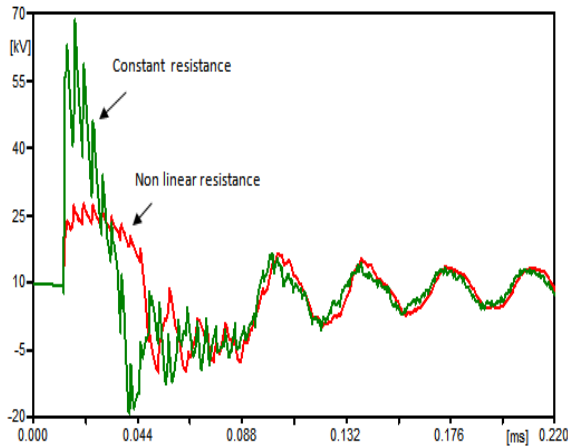
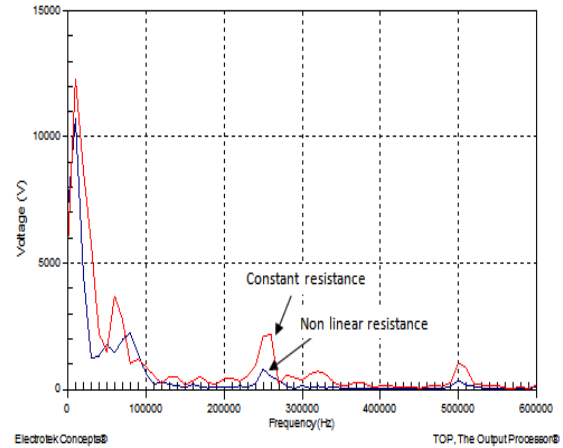


Figure 20. Overvoltage and frequency spectrum @WT#2

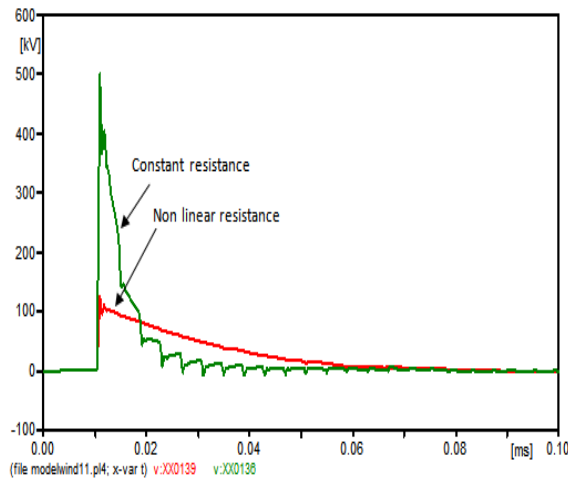


a. Waveforms Comparison at Grid Under Different Ground Model

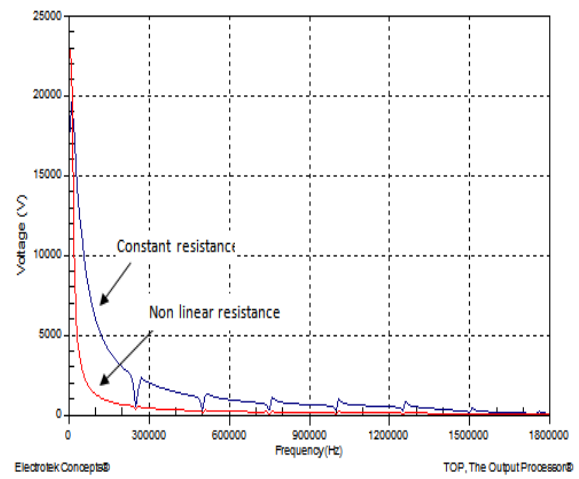


b. Frequency Spectrum Comparison at Grid Under Different Ground Model

Figure 21. Overtoltage and Frequency Spectrum At Grid

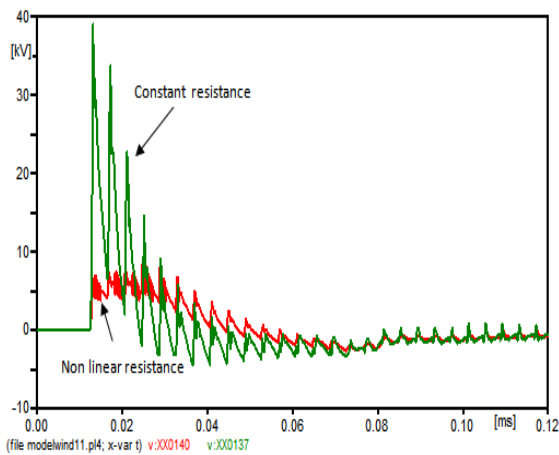


a. GPR Waveform Comparison @ WT#1 under Different Ground Model

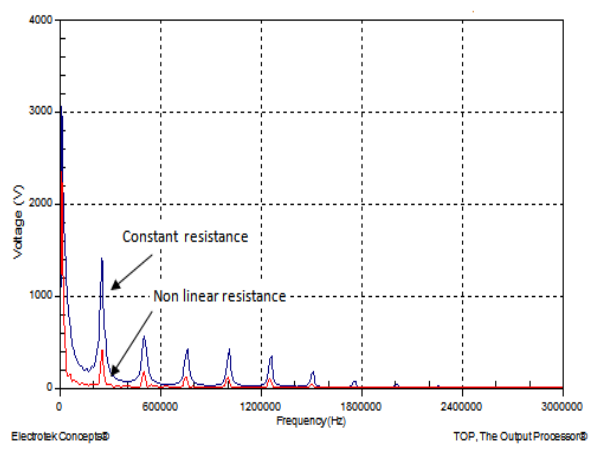


b. Frequency Spectrum Comparison @ WT#1 under Different Ground Model

Figure 22. GPR Waveform and Frequency Spectrum @ WT#1

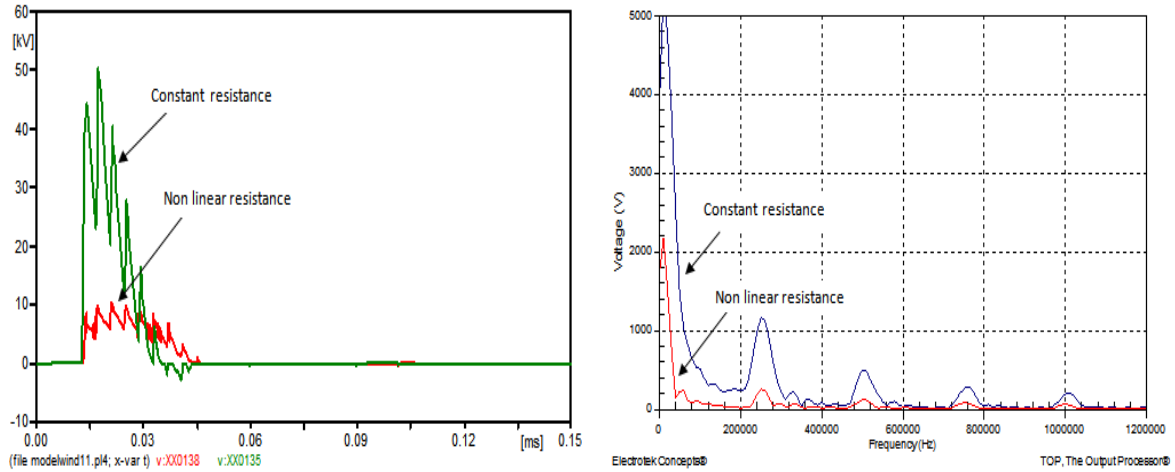


a. Gpr Waveform Comparison @ Wt#2 Under Different Ground Model



b. Frequency spectrum comparison @ WT#2 under different ground model

Figure 23. GPR Waveform and Frequency Spectrum @ WT#2



a. GPR Waveform Comparison At Grid Under Different Ground Model

b. Frequency Spectrum Comparison At Grid Under Different Ground Model

Figure 24. GPR Waveform and Frequency Spectrum at Grid

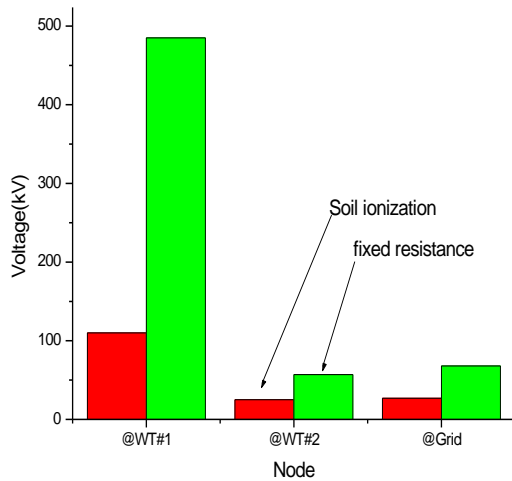


Figure 25. Overvoltage Peak Comparison at Each Node Under Different Cases

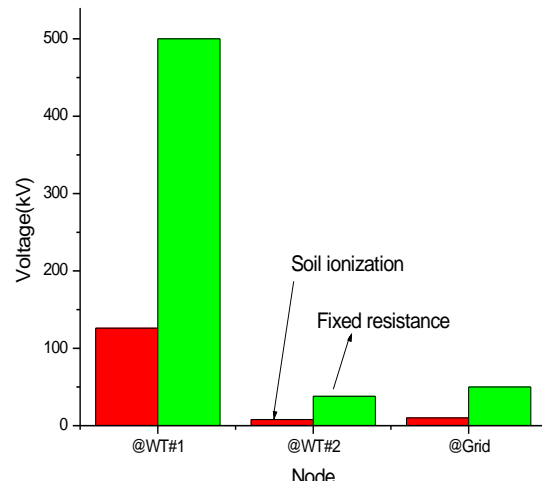


Figure 26. GPR Peak Comparison at Each Node Under Different Cases

5. CONCLUSION

Validation of surge arrester in LV, MV and HV ABB data sheet using ATP/EMTP has been investigated. The impact of the Pinceti and Giannettoni surge arrester and winding stray capacitance transformer model has been carried out. The impact of the soil ionization model has been presented. Performance of wind farm consisting of two wind turbines has been evaluated under lightning strokes. This investigation has been carried out in time domain as well as frequency domain using FFT. All components of the system, under study, are simulated by using ATP/EMTP. The main conclusions obtained from the results are;

In case of the lightning stroke strikes the blade, cause GPR. The increase of the GPR can conduct backflow current to the distribution system. It generates overvoltage on the thunderstruck and neighbor turbines. This can cause damage to the wind farm electrical components.

It is clear that small change in peak value of overvoltages under simple and frequency dependant model. But from frequency content point of view, it can be seen that the amplitude voltage at different frequencies when using simple model is higher than that when using frequency dependant model, due to the

presence of the capacitors in the frequency dependant model. On the other hand, the frequency dependent model considers very high impedance at high frequencies. Therefore, for a better surge analysis of wind farm, the capacitance between winding of transformer model must be taken to get accurate transient results.

The nonlinearity behavior of the grounding resistance can be attributed to the decrease in the grounding resistance within the increase in surge current through it. Therefore, the soil ionization effect is important and should be considered for transient studies especially lightning study.

REFERENCES

- [1] IEC TR 61400-24, "Wind Turbine Generator Systems-Part 24: Lightning Protection", 2002.
- [2] Yasuda Y and Funabashi T," Analysis on Back-Flow Surge in Wind Farms." IPST'07, Lyon, France, June 4-7, 2007.
- [3] J. C. Das, "Transients in Electrical Systems, Analysis, Recognition and mitigation", 2nd Edition, John Wiley and Sons, Inc. 2010.
- [4] Jheng-Lun Jiang, Hong-Chan Chang and Cheng-Chien Kuo," Analysis of transient energy affection for wind farm under lightning," *Energy* 48 (2012) 292e297. www.elsevier.com/locate/energy
- [5] Jheng-Lun Jiang , Hong-Chan Chang , Cheng-Chien Kuo and Cheng-Kai Huang," Transient overvoltage phenomena on the control system of wind turbines due to lightning strike", *Renewable Energy* 57 (2013) 181-189
- [6] Amr M. Abd_Elhady, Nehmdoh A. Sabiha and Mohamed A. Izzularab," Overvoltage Investigation Of Wind Farm Under Lightning Strokes", IET Conference on Renewable Power Generation (RPG, 2011).
- [7] T. Hara, and O. Yamamoto, "Modeling of a Transmission Tower for Lightning-surge Analysis", *IEE Generation, Transmission and Distribution*, Vol. 143, No. 3, pp. 283-289, 1996.
- [8] J. Marti, "Accurate Modeling of Frequency Dependent Transmission Lines in Electromagnetic Transients Simulation", *IEEE Transactions on Power Apparatus and Systems*, PAS-101, No.1, pp. 147-157, 1982.
- [9] A. Greenwood, "Electrical Transients in Power Systems", 2nd Edition, John Wiley and Sons, Inc. 1991.
- [10] IEEE working Group 3.4.11, Application of Surge Protective Devices Subcommittee Surge Protective Devices Committee, "Modeling of Metal Oxide Surge Arresters", *IEEE Transactions on Power Delivery*, Vol. 7, No. 1, pp. 302-309, January 1992.
- [11] P. Pinceti and M. Giannettoni, "A Simplified Model for Zinc Oxide Surge Arresters", *IEEE Transactions on Power Delivery*, Vol. 14, No. 2, PP. 393-398, April 1999.
- [12] M. agro, M. Giannettoni and P. Pinceti, "Validation of ZnO Surge Arresters Model for Overvoltage Studies", *IEEE Transactions Power Delivery*, Vol. 19, No. 4, PP. 1692-1695, October 2004.
- [13] Nehmdoh A. Sabiha and Matti Lehtonen, "Lightning-Induced Overvoltages Transmitted Over Distribution Transformer With MV Spark-Gap Operation—Part II: Mitigation Using LV Surge Arrester" *IEEE TRANSACTIONS ON POWER DELIVERY*, VOL. 25, NO. 4, OCTOBER 2010
- [14] Surge Arresters, Datasheet, www.abb.com/arrestersonline.
- [15] Amr M. Abd-Elhady, Nehmdoh A. Sabiha and Mohamed A. Izzularab" *Evaluation of Different Grounding Models for Studying Backflow Current-Overvoltages in Wind Farm*" International Middle East Power Systems Conference (MEPCON'12) 23-25 December 2012, Cairo, Egypt.
- [16] ANSI/IEEE Std 80-1986" AC SUBSTATION GROUNDING"